ACS APPLIED MATERIALS & INTERFACES

Research Article

www.acsami.org

Poly(Ethylene Oxide) Functionalized Polyimide-Based Microporous Films to Prevent Bacterial Adhesion

Aránzazu Martínez-Gómez,[†] Cristina Alvarez,[†] Javier de Abajo,[†] Adolfo del Campo,[‡] Aitziber L. Cortajarena,[§] and Juan Rodriguez-Hernandez*[,†]

[†]Instituto de Ciencia y Tecnología de Polímeros (ICTP-CSIC), C/Juan de la Cierva 3, 28006-Madrid, Spain

[‡]Instituto de Cerámica y Vidrio (ICV-CSIC), C/Kelsen 5, 28049-Madrid, Spain

[§]Instituto Madrileño de Estudios Avanzados en Nanociencia (IMDEA-Nanociencia), Cantoblanco, and CNB-CSIC-IMDEA Nanociencia Associated Unit "Unidad de Nanobiotecnología", 28049-Madrid, Spain

ABSTRACT: Preventing microbial adhesion onto membranes is a crucial issue that determines the durability of the membrane. In this Research Article, we prepared aromatic polyimides (extensively employed for the elaboration of ultrafiltration membranes) containing PEO branches. Four polyimide-*g*-PEO copolymers were prepared from 6F dianhydride and a novel aromatic diamine containing PEO-550 side groups. The copolymers were designed to have variable PEO content, and were characterized by their spectroscopic and physical properties. The Breath Figure technique was successfully applied to create an ordered surface topography, where the PEO chains were preferentially located on the surface of the micrometer size holes. These unique features were explored to reduce bacterial adhesion. It was established that surface modified polyimide membranes have a high resistance to biofouling against *Staphylococcus aureus*. In particular, we observed that an increase of the PEO the content in the copolymer produced a decrease in the bacterial adhesion.

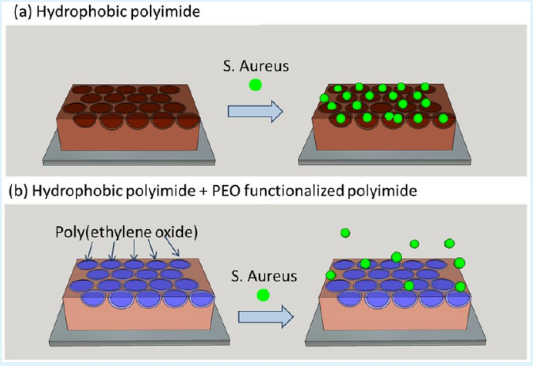

KEYWORDS: *Breath Figure, antifouling surfaces, polyimide membranes, surface functionalization, bacterial adhesion*

INTRODUCTION

Microporous interfaces have found interest for multiple applications in a variety of fields ranging from optics to biomedical applications.[1−3] For instance, porous materials with pore dimensions comparable to the wavelength of visible light are of interest as photonic band-gaps and optical stop-bands. Other than the two mentioned applications, porous materials with cavities in the micrometer size range are interesting in such applications as catalysis, as sensors, scaffolds for composite materials, selective transportation, in insulation processes, or for membrane preparation.[4−9]

Porous structures with micrometer or even submicrometer dimensions have been typically prepared using different approaches that requires the use of templates.[10,11] Currently employed methodologies include the use of templates, such as ordered arrays of colloidal particles to produce inverse opal structures,[12−16] from transformed polymeric sphere arrays,[17,18] using emulsion droplets as templates,[19] employing natural biological templates,[20−23] by phase inversion,[24] self-organized surfactants,[25] and microphase separated or electric-field-induced block copolymers patterning.[26−28] Other alternatives include direct writing of polymer patterns,[29] the use of photo- or electrochemically polymerizable precursors[30] or soft lithographic methods.[31]

In addition to the above-mentioned strategies, an alternative approach is the Breath Figure (BF) templating method in which the template consists of an ordered array of water droplets that may be removed by simple evaporation.[5−9,32−34] As a consequence of its simplicity this techniques is currently one of the most widely employed methods for the fabrication of nano- and microporous polymer films with different surface functionalities.[35,36] Several significant advantages justify its extensive use. On the one hand, the self-removal of the template favors a reduction on the production time and cost. On the other hand, BF allows the employment of a large variety of materials ranging from polymers (including blends of different polymers) to hybrid nanocomposites thus leading to porous films having a broad range of properties. As will be evidenced in this manuscript, the dimensions and shape of the pores, and functionality inside and outside of the pores are determined by the following parameters: temperature, air humidity, solvent, polymer concentration,, or the presence of functional groups in the polymer. Thus, the pore characteristics could be easily manipulated by controlling these parameters.

Received: February 16, 2015
Accepted: April 24, 2015
Published: April 24, 2015

DOI: 10.1021/acsami.5b01525
ACS Appl. Mater. Interfaces 2015, 7, 9716−9724

Microporous polymeric surfaces and in particular those applied for water filtration exhibit microbiological contamination during their usage. The microorganism adhesion to polymeric membranes causes changes in the separation processes and has associated secondary processes including the contamination by the metabolism products.[37] Among others, the result of this contamination may provoke the destruction of the membrane surface, which increases the manufacturing costs and reduces the operating life for the membrane.

Within this context, several alternatives have been explored to design microporous surfaces with either antibacterial or antifouling properties. Some strategies have been developed to reduce the contamination of the surfaces by introducing bioactive molecules with antibacterial activity. One of the most extended approach is the chemical modification of the surfaces to introduce ionic substances,[38] for instance, by immobilization of bactericidal agents. Among them tertiary amines,[39] antimicrobial peptides,[40] pyridinium cations,[41,42] or guanidine groups have been reported.[37] Other research groups immobilized antifouling molecules such as zwitterions[43,44] or Tween 20[45] among others.[46] A particularly interesting alternative consists on the design of a microporous surfaces having poly(ethylene oxide) (PEO) moieties. In fact, PEO has been extensively employed because of its antifouling properties in different biomedical applications ranging from implants to biosensors or nanoparticles.[47] For this reason, PEO has often been called the "gold standard" of antifouling polymers.[48,49] The immobilization of PEO typically has been achieved by chemical reactions on the polymer surface.[50−53] For instance, Xue et al.[51] and Prince et al.[52] employed poly(acrylonitrile-*co*-maleic acid) (PANCMA) as a linker to chemically attach PEO and silver to PES hollow fiber membrane. Yu et al.[53] employed long-wavelength UV irradiation to graft PEGMA onto polysulfone (SPF) ultrafiltration membrane using benzophenone as initiator. These are two selected examples from a large number of studies in which was evidenced the need to modify the interfacial chemical composition of microporous surfaces in order to avoid microorganism adhesion.[54−59] Another alternative to fabricate membranes with controlled surface chemistry is based on the use of functional copolymers for the preparation of the membranes. In this context, amphiphilic macromolecules made from polyamide-*g*-PEO copolymers have been recently prepared by our group by using polycondensation reactions monomers containing pendent PEO chains.[60]

On the basis of this second strategy, in this Research Article, we report the preparation of microporous surfaces based on polyimide copolymers having pendant poly(ethylene oxide) (PEO) chains, that is, polyimide-*g*-PEO copolymers. Previous studies reported the use of polyimides for the preparation of porous films by the Breath Figure approach.[61−65] However, the chemical design of polyimides in order to introduce hydrophilic functional groups with antifouling properties is unprecedented. The amphiphilic nature of the resulting polymer would favor the water condensation and thus the formation of ordered porous films. Moreover, PEO would have two additional roles. On the one hand the incorporation of PEO facilitates the solution in volatile solvents such as chloroform required for the preparation of porous films by the BFs approach. On the other hand, as depicted above PEO would work as antifouling compound to prevent the adhesion of microorganisms onto the porous films. Finally, we explored the adhesion of *S. aureus* on the porous films as a function of the PEO included in the material.

EXPERIMENTAL SECTION

Materials. Chloroform ($CHCl_3$) was supplied by Scharlau and round glass coverslips of 12 mm diameter were obtained from Ted Pella Inc. All solvents and chemicals (e.g., 3,5-dinitro-benzoyl chloride (Sigma-Aldrich)), were purchased as reagent degree products and used without further purification unless detailed. 1,3.5-trimethyl-*m*-phenylenediamine (**3MeMPD** Aldrich) was purified by sublimation. Hexafluoroisopropylidene diphthalic anhydrided (**6FDA** Aldrich) was purified by sublimation. Chlorine-terminated PEO500 monomethyl ether was prepared following previously reported procedures.[66]

Characterization. The ^1H and ^{13}C NMR spectra were registered at room temperature in $CDCl_3$ solution in Varian INOVA-300. Chemical shifts are reported in parts per million (ppm) using as internal reference the peak of the trace of deuterated solvent (δ 7.26). The number-average molecular weight (M_n) and polydisperstiy index (PD = M_w/M_n) were measured with a chromatographic system (Waters Division Millipore) equipped with a Waters model 2414 refractive-index detector. Dimethylformamide (Multisolvent HPLC, Scharlau) containing 0.1% of LiBr, was used as the eluent at a flow rate of 0.7 mL min^{-1} at 70 °C. Styragel packed columns (HR2 and HR5, Waters Division Millipore) were used. Polystyrene standards (Polymer Laboratories, Laboratories, Ltd.) between 5.7×10^5 and 5.8×10^2 g mol^{-1} were used to calibrate the columns.

Scanning electron microscopy (SEM) micrographs were taken using a Philips XL30 with an acceleration voltage of 25 kV. The samples were coated with gold−palladium (80/20) prior to scanning.

The topography, chemical composition and distribution of the different components of the blends on the polymeric films were determined using Confocal Raman Microscopy integrated with atomic force microscopy (AFM) on a CRM-Alpha 300 RA microscope (WITec, Ulm, Germany) equipped with Nd:YAG dye later (maximum power output of 50 mW power at 532 nm). The Raman spectra were taken point by point with a step of 100 nm.

Synthesis of the Polyimide Graft Polymers. *Synthesis of 3,5-Diamino(ω-Methy-6l-PEO) Benzoic Ester (PEO500).* 3,5-Dinitrobenzoyl chloride (30.0 g, 0.13 mol) was added in dropwise fashion to a mixture of chloroform (100 mL), PEO 550 (72.0 g, 0.13 mmol), and pyridine (12 mL, 0.15 mol) at 0 °C. The reaction was allowed to warm up to room temperature (RT) and stirred for 15 min, followed by heating at reflux for 4 h, and then cooled down to RT again. Finally, the reaction was washed with water several times and dried over anhydrous magnesium sulfate, and the product of reaction was concentrated under reduced pressure. The resulting solid was purified by silica chromatography using dichloromethane, followed by dichloromethane/methanol (10/0.5) as eluent to afford the dinitro intermediate as a yellow oil.

Yield: 90%. ^1H NMR ($CDCl_3$, ppm): δ = 3.36 (s, 3H, $OC\underline{H}_3$), 3.50−3.90 (m, 52 H, $OC\underline{H}_2$), 4.58 (t, 2H, $C(=O)OC\underline{H}_2$), 9.15 (d, 2H, $C\underline{H}CC=O$), 9.20 (t, 1H, $O_2NCC\underline{H}CNO_2$). ^{13}C NMR ($CDCl_3$, ppm): δ = 59.2 ($O\underline{C}H_3$), 66.0 ($C(=O)O\underline{C}H_2$), 68.9 ($C(=O)OCH_2\underline{C}H_2$), 70.7 ($O\underline{C}H_2$), 72.1 ($\underline{C}H_2OCH_3$), 122.6 ($O_2NC\underline{C}HCNO_2$), 129.8 ($\underline{C}HCC=O$), 134.0 ($\underline{C}C=O$), 148.8 ($\underline{C}NO_2$), 162.7 ($\underline{C}=O$).

A solution of 5.0 g of dinitro intermediate in tetrahydrofuran (50 mL) was charged into a Parr reactor, followed by addition of palladium-on-charcoal (10% Pd basis, 100 mg). Reactor was purged with hydrogen gas twice at 3 atm. Hydrogen pressure was maintained in the Parr autoclave until hydrogen consumption ceased (24 h). The reaction was then filtered through a plug of Celite to remove Pd/C and washed afterward with tetrahydrofuran. The diamine *m*PD-PEO550 was concentrated under reduced pressure to give orange oil that is used without further purification.

Yield :95%. ^1H NMR ($CDCl_3$, ppm): δ = 3.36 (s, 3H, $OC\underline{H}_3$), 3.50−3.85 (m, 52 H, $OC\underline{H}_2$), 4.40 (t, 2H, $C(=O)OC\underline{H}_2$), 6.50 (broad s, 1H, $O_2NC=C\underline{H}-CNO_2$), 6.91 (t, 2H, $C\underline{H}CC=O$). ^{13}C NMR ($CDCl_3$, ppm): δ = 59.2 ($O\underline{C}H_3$), 68.2 ($C(=O)O\underline{C}H_2$), 69.4

DOI: 10.1021/acsami.5b01525
ACS Appl. Mater. Interfaces 2015, 7, 9716−9724

Table 1. Characteristics of the PEO-Polyimides Synthesized in This Study As a Function of the Feed Composition[a]

	feed composition						
polymer	PEO 550 (**1**)	3MeMPD (**2**)	6FDA (**3**)	M_n (kDa)	PD	T_g (°C)	WCA[a] (deg)
P1	0	1	1	177	1.5	375	116
P2	0.5	0.5	1	109.1	1.5	90	105
P3	0.75	0.25	1	62.7	1.8	45	98
P4	1	0	1	91	2.6	n.d.	58

[a]WCA: water contact angles of the porous films prepared from the polymers P1−P4.

Scheme 1. Synthetic Route Employed to Obtain Polyimides with PEO-Lateral Chains Involving the Formation of a Polyamic Acid (Step 1) and the Cyclodehydration to Obtain the Final PEO-Grafted Polyimide (Step 2)

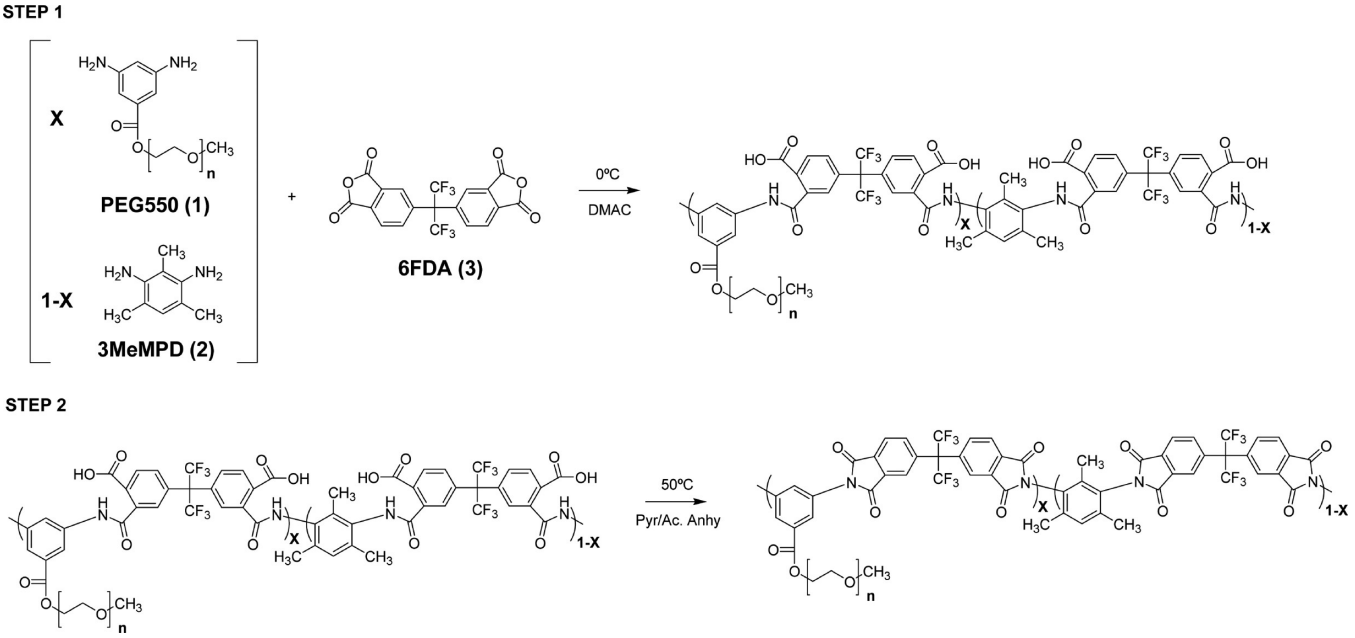

(C(=O)OCH$_2$CH$_2$), 70.7 (OCH$_2$), 72.1 (CH$_2$OCH$_3$), 107.5 (O$_2$NCCHCNO$_2$), 108.4 (CHCC=O), 132.1 (CC=O), 146.5 (CNH$_2$), 166.9 (C=O).

Synthesis of Polyimide Graft Copolymers. The general procedure is as follows: In a three-necked flash, equipped with a mechanical stirrer and nitrogen inlet, diamine or a mixture of diamines (8.0 mmol) was dissolved in anhydrous *N,N*-dimethylacetamide (20 mL). The solution was cooled down to 0 °C, and dianhydride 6FDA (8.0 mmol) was then added. The stirring was continued for 15 min at that temperature and for further 12 h at RT to yield a viscous solution of poly(amic acid). Subsequently, a mixture of acetic anhydride (24.0 mmol)/pyridine (24.0 mmol) was added, and the solution was stirred for 6 h at RT and 1 h at 60 °C to promote the imidation. After it was cooled down to RT, the polymer was poured dropwise into water, washed several times with water and dried over P_2O_5 under vacuum at 60 °C for 24 h. The polyimide 6FDA-*m*PD-PEO550 (**P4**) was synthesized with the same procedure but it was directly precipitated in ethyl ether.

*6FDA-3MemPD (**P1**).* ^{1}H NMR (DMSO-d_6, ppm): δ = 1.91 (s, 3H, H$_l$), 2.13 (s, 6H, H$_m$), 7.32 (s, 1H, H$_k$), 7.92 (s, 4H, H$_h$ and H$_j$), 8.16 (d, 2H, H$_i$). FT-IR (film, cm^{-1}): ν 2930 (aliphatic C−H str.), 1787 (C=O asym. str.), 1723 (C=O imide sym. str.), 1457 (CH$_2$ sym. def. and CH$_3$ asym. def.), 1355 (C−N−C stretching), 723 (imide ring deformation).

*6FDA-3MemPD/6FDA-mPDPEO550 (50/50) (**P2**).* ^{1}H NMR (DMSO-d_6, ppm): δ = 1.92 (s, 1.5H, H$_l$), 2.13 (s, 3H, H$_m$), 3.21 (s, 1.5H, H$_e$), 3.36−3.90 (m, 24 H, H$_b$, H$_c$, and H$_d$), 4.47 (s, 1H, H$_a$), 7.33 (s, 0.5H, H$_k$), 7.90 (m, 4.5H, H$_f$, H$_h$, and H$_j$), 8.20 (m, 3H, H$_g$, and H$_i$). FT-IR (film, cm^{-1}): ν 2870 (aliphatic C−H str.), 1784 (C=O asym. str.), 1723 (C=O imide sym. Str. and C=O ester str.), 1457 (CH$_2$ sym. def. and CH$_3$ asym. def.), 1355 (C−N−C stretching), 719 (imide ring deformation).

*6FDA-3MemPD/6FDA-mPDPEO550 (50/25) (**P3**).* ^{1}H NMR (DMSO, ppm): δ= 1.92 (s, 0.75H, H$_l$), 2.15 (s, 1.5H, H$_m$), 3.21 (s, 2.25H, H$_e$), 3.36−3.90 (m, 35H, H$_b$, H$_c$, and H$_d$), 4.46 (s, 1.5H, H$_a$), 7.33 (s, 0.25H, H$_k$), 7.90 (m, 4.75H, H$_f$, H$_h$, and H$_j$), 8.20 (m, 3.5H, H$_g$ and H$_i$). FT-IR (film, cm^{-1}): ν 2870 (aliphatic C−H str.), 1784 (C=O asym. str.), 1723 (C=O imide sym. Str. and C=O ester str.), 1457 (CH$_2$ sym. def. and CH$_3$ asym. def.), 1355 (C−N−C stretching), 719 (imide ring deformation).

*6FDA-mPDPEO550 (**P4**).* ^{1}H NMR (DMSO-d_6, ppm): δ= 3.22 (s, 3H, H$_e$), 3.40−3.85 (m, 46 H, H$_b$, H$_c$, and H$_d$), 4.47 (s, 2H, H$_a$), 7.80 (s, 2H, H$_h$), 7.91 (s, 1H, H$_f$), 7.97 (d, 2H, H$_j$), 8.20 (m, 4H, H$_g$, and H$_i$). FT-IR (film, cm^{-1}): ν 2870 (aliphatic C−H str.), 1785 (C=O asym. str.), 1723 (C=O imide sym. str. and C=O ester str.), 1457 (CH$_2$ sym. def. and CH$_3$ asym. def.), 1353 (C−N−C stretching), 1090 (O−C−O asym. str.), 719 (imide ring deformation). Other characterization results such as viscosity and glass transition temperatures for all the four polymers are listed in Table 1.

Preparation of the Porous Films by the Breath Figure Technique. The preparation of the porous films was carried out from chloroform solutions by casting onto glass wafers under high controlled humidity (relative humidity (RH) = 80%−99%) inside of a closed chamber at room temperature. For this study we employed polymer solutions ranging from 11 to 30.0 mg mL^{-1}. $CHCl_3$ was used as solvent in all the cases. In addition to the polyimides with variable amount of PEO (see Table 1) we prepared porous films from blends of polymer (1 and 2) with either 10 or 20 wt % of polymer 2 and 90 or 80 wt % of polymer 1, respectively. These films were prepared from 10 mg mL^{-1} solutions in $CHCl_3$.

DOI: 10.1021/acsami.5b01525
ACS Appl. Mater. Interfaces 2015, 7, 9716−9724

Bacterial Adhesion Experiments. *S. aureus* strain RN4220 carrying the plasmid pCN57 for Green fluorescent protein (GFP) expression (generous gift from Iñigo Lasa's Laboratory at Instituto de Agrobiotecnología, UPNA-CSIC-Gobierno de Navarra) was grown overnight at 37 °C in Luria–Bertani (LB) media with erythromycin (10 μg/mL). The cells were centrifuged and washed three times in PBS buffer (150 mM NaCl, 50 mM Na-phosphate pH 7.4). The solution was adjusted to a cell concentration that corresponds to an optical density (OD) at 600 nm of 1.0 using an UV–vis Varian Cary 50 spectrophotometer.

The different patterned polymeric surfaces were incubated during 1 h with the bacterial suspension at OD = 1.0 in PBS buffer with 0.05% Tween 20 to allow for bacteria adhesion. After incubation the surfaces were washed with PBS three times during 15 min in order to remove the not adhered bacteria.

Bacteria adhesion to the different surfaces was monitored and quantified by fluorescence microscopy using a Leica DMI-3000-B fluorescence microscope using the green fluorescence signal of the cells. Images were acquired using ×20 magnification and the corresponding set of filters for imaging green fluorescence and bright field.

RESULTS AND DISCUSSION

Synthesis of the Polyimides with Hydrophilic PEO Pendant Groups. The polyimide-*g*-PEO copolymers were prepared by polycondensation reactions between the fluorinated dianhydride hexafluoroisoprolydene diphthalic (dianhydride 6F), and variable ratio of two aromatic diamines: 2,4,6-trimethyl-m-phenylenediamine (3MeMPD) and 5-carboxy-PEO-m-phenylenediamine (PEO550).

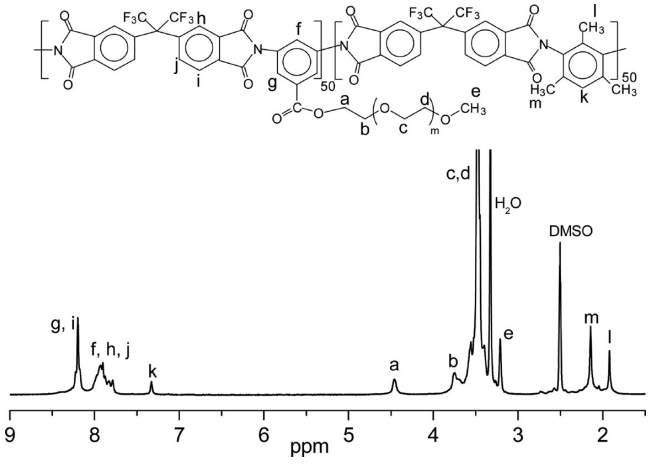

Figure 1. Illustrative ^{1}H NMR spectrum of copolymer **P2**.

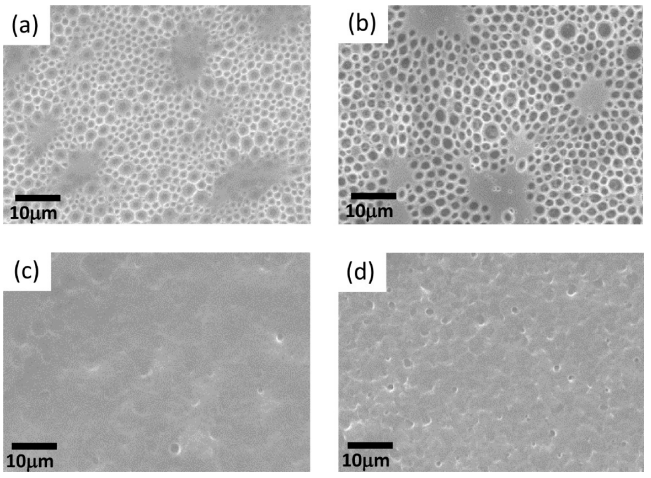

Figure 3. SEM images of the porous films obtained for polymers (a) **P1**, (b) **P2**, (c) **P3**, and (d) **P4**. For the preparation of these films a 10 mg/mL polymer solutions and 80% rh moist environment were employed.

The polycondensation reaction was performed by a two-step methodology in solution using *N*,*N*-dimethylacetamide (DMAC) at low temperature. The corresponding polyamic-acid precursor was formed in the first step, and the final polyimide was obtained by cyclodehydration promoted by the system pyridine-acetic anhydride at 50 °C in the second step. The polyimide without PEO was attained in quantitative yield, and the yields of the copolymers were not lower than 85%. The scheme of the reaction is depicted in Scheme 1, and the results of the synthesis are summarized in Table 1.

Polymers were characterized both by FT-IR and ^{1}H NMR. An illustrative example of the ^{1}H NMR spectrum is depicted in Figure 1 of copolymer **P2**, having 0.5:0.5 ratio of the two diamines. In this spectrum, the signals between 5.0 and 3.0 ppm are due to aliphatic protons of PEO550 segments. In addition,

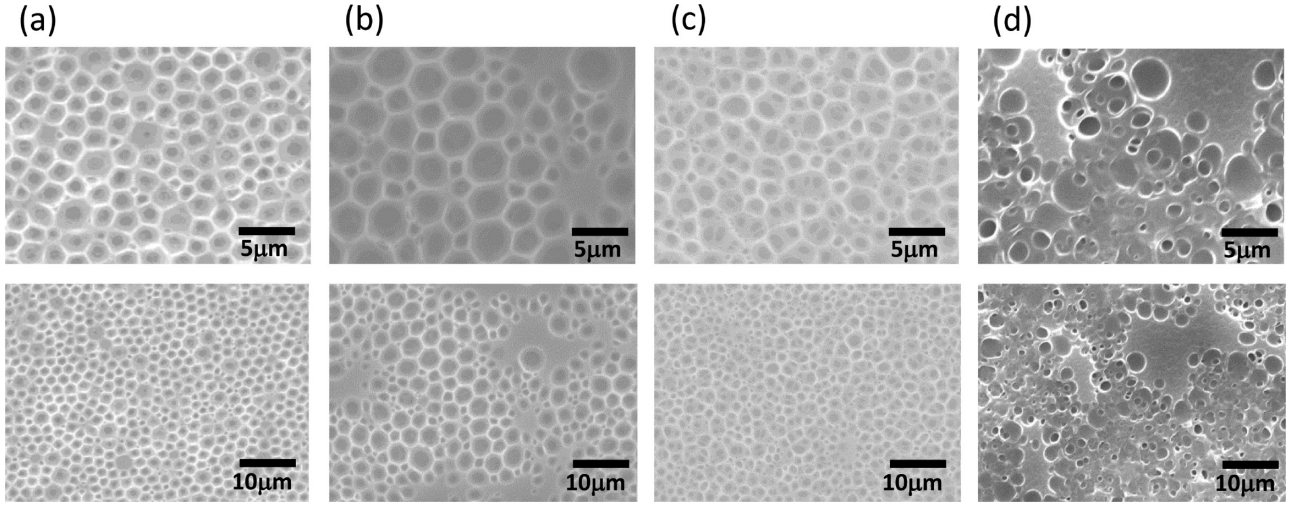

Figure 2. SEM images of the porous films obtained for polymers (a) **P1**, (b) **P2**, (c) **P3**, and (d) **P4**. For the preparation of these films a 10 mg/mL polymer solutions and 99% rh moist environment were employed.

DOI: 10.1021/acsami.5b01525
ACS Appl. Mater. Interfaces 2015, 7, 9716–9724

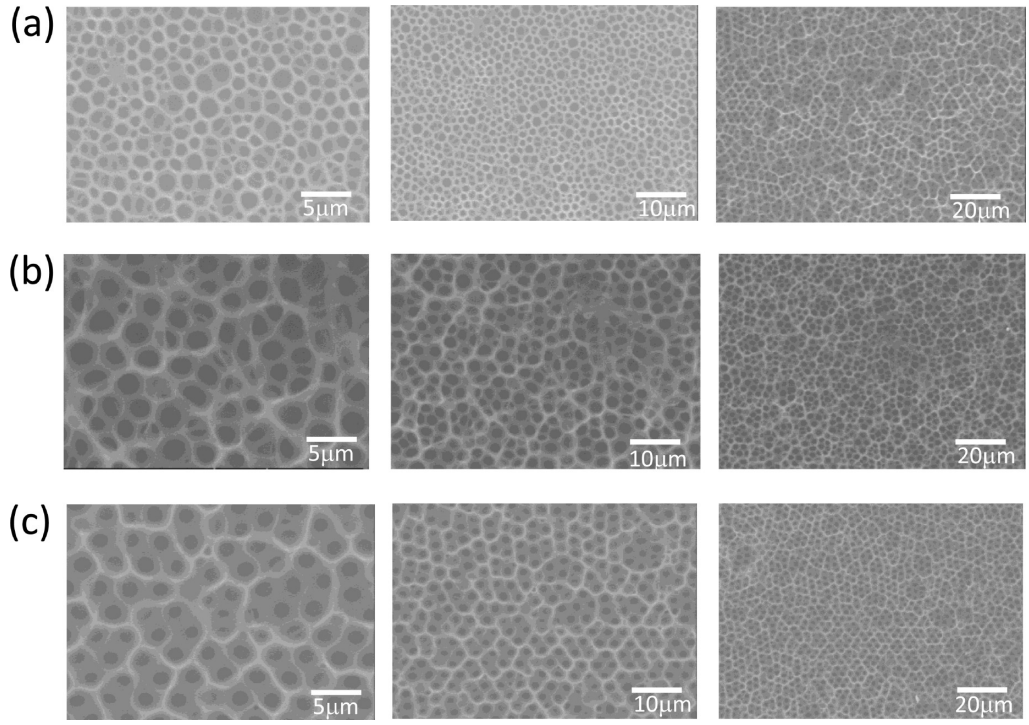

Figure 4. SEM images of the porous films obtained for blends for polymer **P1** and **P2** at three different wt % ratio: (a) 100/0 **P1**/**P2**, (b) 90/10 **P1**/**P2**, and (c) 75/25 **P1**/**P2**. The conditions selected were 10 mg/mL polymer solutions and 90% rh moist environment.

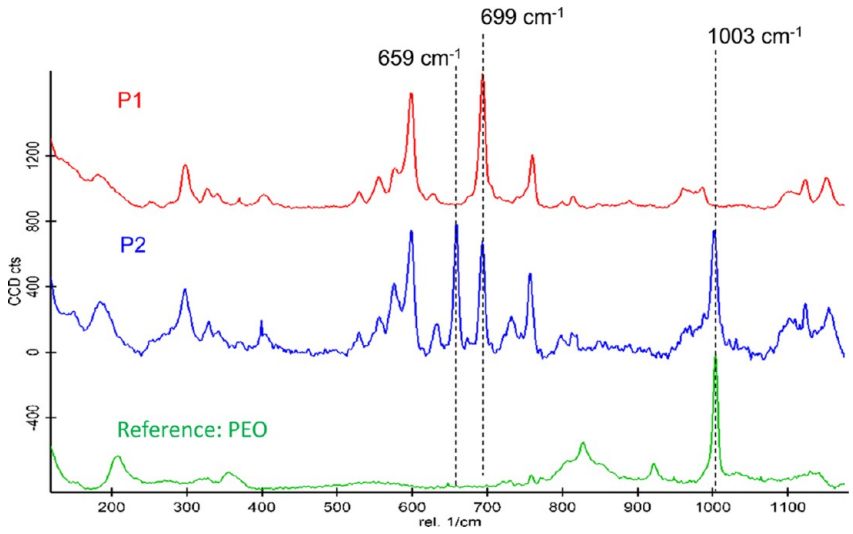

Figure 5. Raman spectra of the polyimides having either 0% of PEO (**P1**) or 50% of PEO (**P2**) and a PEO employed as reference.

two signals around 2.0 ppm (H_m and H_i) can be assigned to the methyl groups of the diamine 3MemPD in the copolymer whereas the signals of aromatic protons appear between 7.0 and 8.5 ppm. The composition calculated from the areas under the signals at 4.5 ppm (corresponding to the protons on methylene a), and that of peak at 2.2 ppm (corresponding to protons of aromatic methyl groups (protons m)), agreed with the feed composition.

Porous Films Prepared from Polyimides-PEO: Honeycomb Formation. The formation of porous interfaces was accomplished by the Breath Figure approach. For that purpose, the polymer was dissolved in a volatile solvent (in this case $CHCl_3$) varying the concentration between 1 and 30 mg/mL. The polymer solutions (30−60 μL) were dropped onto glass covers that were previously cleaned and were closed in a vessel chamber under controlled humidity. Once a precise amount of the solution was deposited onto the glass slides, the solvent was allowed to evaporate within the chamber. During the evaporation of the solvent, the water vapor condensed at the solution surface as a consequence of the significant decreased of the solvent temperature. Condensation throughout the evaporation induced the formation of water droplets that grew until the solvent was completely evaporated. Upon complete evaporation of the solvent, the water droplets formed by condensation equally evaporated leaving pores at the surface. Many studies have explained the formation of these structures and the factors that regulate both the regularity of the pores and their size. Among others the humidity and the

DOI: 10.1021/acsami.5b01525
ACS Appl. Mater. Interfaces 2015, 7, 9716−9724

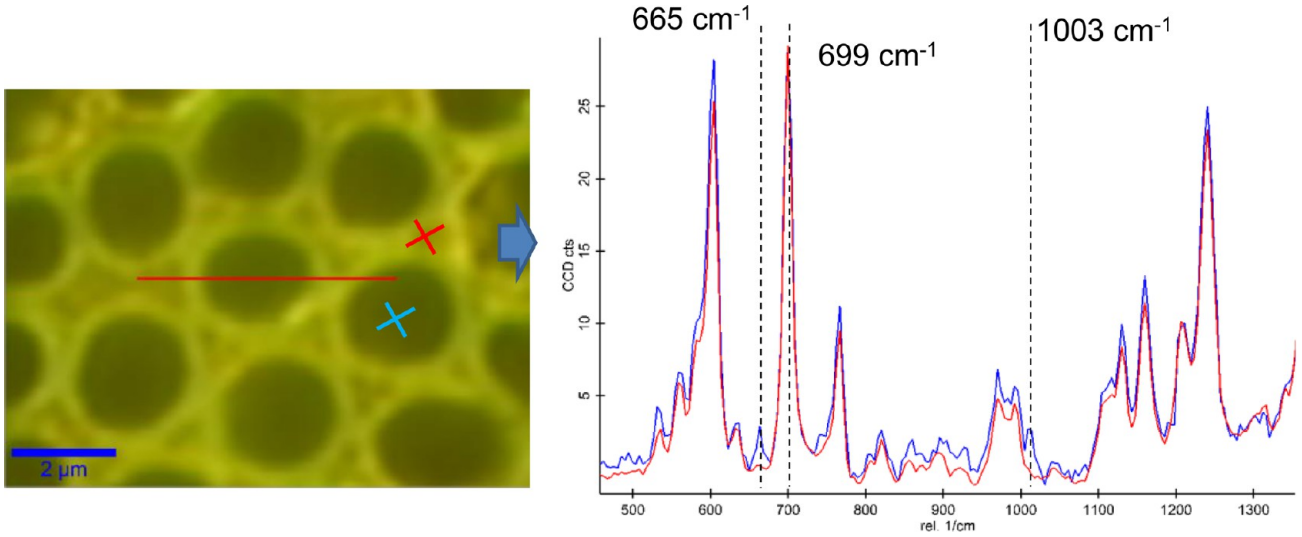

Figure 6. Left: Optical image of the porous films prepared from the blend 90/10 **P1**/**P2**. Right: Raman spectra obtained in two different areas, that is, inside of the pores (red curve) and outside of the pore (blue curve).

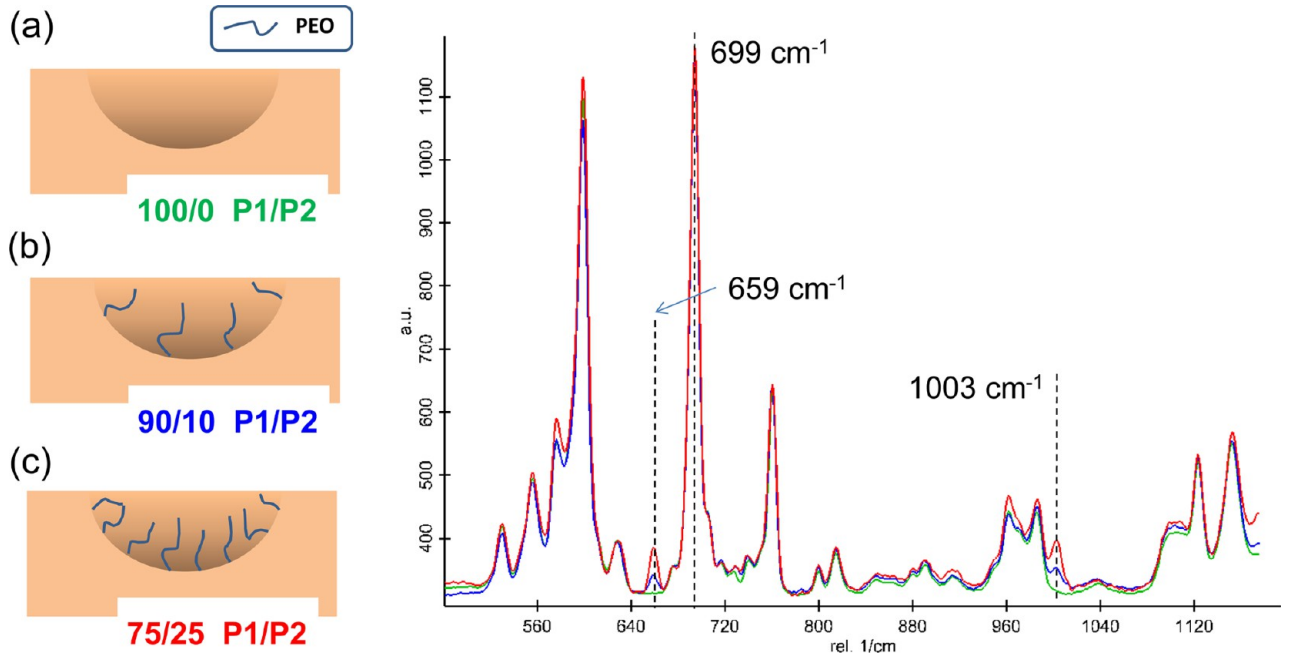

Figure 7. Left: Schematic illustration of the chemical composition of the honeycomb films and the distribution of the components **P1** (beige color) and **P2** (blue color) of the blends employed for the film preparation. Right: RAMAN spectra obtained in the center of the pores of the honeycomb films prepared from (a) only **P1** (green), (b) blend of **P1**/**P2** (90:10) (blue), and (c) blend of **P1**/**P2** (75:25) (red).

concentration of the polymer solution have been reported to clearly influence the pore formation. In addition, the presence of polar groups on the copolymer structure favors the water condensation and thus the pore formation but if the amount of polar groups is too high may induce coagulation.[5−8]

In this study we first optimized the surface patterns by varying different parameters. First the amount of PEO included in the copolymer. As depicted in Figure 2, for these experimental conditions a rather regular structure was obtained for **P1** with average pores sizes of 2 μm. The rest of the copolymers employed led to disordered structures in which the coagulation phenomenon could be clearly observed. Reduction of the relative humidity did not improve the regularity of the pores obtained (see Figure 3). Decrease of the relative humidity to 80%, **P1** and **P2** produced heterogeneous porous films with areas exhibiting pores with different degree of order and flat areas where the condensation process did not occur. In **P3** and **P4** irregular coagulation may be accompanied by partial solution of the material and as a result the films were rather irregular. The contact angles of these films are shown in Table 1. These values confirmed that the increase in the content of PEO, from polymer **P1** to copolymer **P4**, led to an increasing degree of hydrophilicity.

Considering both the difficulty to obtain ordered porous films with copolymers with PEO and the large order obtained for the copolymer without PEO (**P1**) several blends of **P1** and **P2** polymers were prepared. According to previous studies, blending may have advantages over the employment of pure

DOI: 10.1021/acsami.5b01525
ACS Appl. Mater. Interfaces 2015, 7, 9716−9724

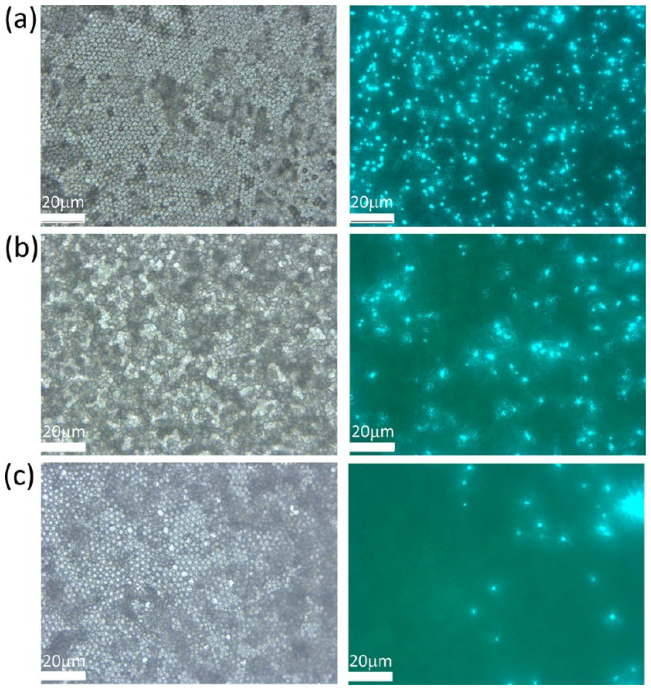

Figure 8. Bacterial adhesion tests on honeycomb structured films prepared from (P1), and blends of **P1** and **P2** having different wt % ratio: (a) 100/0 **P1**/**P2**, (b) 90/10 **P1**/**P2**, and (c) 75/25 **P1**/**P2** (scale bar 20 μm).

functional copolymers. Blending allows the control of the chemical composition of the pore while maintaining the composition of the rest of the material. More precisely, as previously reported, blending functional additives and non-functional polymers (matrix) produces a phase separation induced by the affinity of the polar component toward the condensed water droplet. As a consequence, polar groups enriched the surface of the pore while the external surface (in contact with air during the evaporation process) remains hydrophobic.[7,9] In the present case, the possibility of blending may have several important advantages. First, as a result of the phase separation the hydrophilic component may segregate selectively toward the pore inner cavity. Thus, the hydrophobic component (**P1** in this case) will ensure the structural resistance to water exposure since the areas between the pores formed by **P1** will not swell. More interestingly, the pores will be decorated with **P2** having PEO as side chains. PEO is known to prevent microbial adhesion on different substrates. Thus, this interesting feature is expected to reduce the microorganism adhesion.

The preparation of porous films with the blends was carried out using $CHCl_3$ and variable amounts of **P1** and **P2**. By using 10 mg/mL of polymer solutions and a relative humidity of 90%, two different blends were prepared having either 10 or 25 wt % of **P2** and 90 or 75 wt % of **P1** respectively. As control porous films of **P1** under the same conditions were prepared (Figure 4). Independently of the amount of **P2** the resulting surfaces led to regular porous films with pore sizes between ~2−3 μm.

Raman Confocal Imaging: Elucidating the Position of the Blend Components within the Porous Film. Confocal Raman spectroscopy allowed us to elucidate the precise position of each component on the porous film. Figure 5 depicts the Raman spectra obtained for **P1** and **P2**, and a linear PEO control. It can be observed a signal at 1003 cm^{-1} that can be identified in **P2** and is absent in **P1**. Thus, this signal corresponds to the PEO lateral chains and will be employed as reference.

The variation of the intensity of this signal will allow us to determine the relative concentration of the two components. Figure 6 includes an optical image of a porous surface in which Raman spectra were acquired at two different positions inside and outside of the pores (Figure 6b). The Raman spectra indicate a clear variation in the chemical composition between these two positions. In particular, the presence of the band at 1003 cm^{-1} assigned to the PEO side chains has been exclusively found inside of the pores. This fact indicates the enrichment of the partially hydrophilic polyimide toward the pore during the water condensation. More interestingly, the amount of hydrophilic PEO segments within the pores could be also varied. In Figure 7 are depicted the Raman spectra obtained inside of the pores for two different blends having 10 and 25 wt % of **P2** and the Raman spectra of **P1** employed as reference. Following the band at 1003 cm^{-1} it can be evidenced a direct relation between the intensity of this band (and thus the pore chemical composition) and the P2 wt % of the blend employed for the preparation of the porous films. Thus, films prepared from the blend 75/25 **P1**/**P2** exhibited the largest band intensity. A smaller intensity was observed in the spectrum of the 90/10 **P1**/**P2** blends. Finally, this signal disappeared in the **P1** spectrum.

Bacterial Adhesion as a Function of the Pore Composition. The porous surfaces having different amount of PEO inside of the pores may potentially be employed to prevent bacterial adhesion. The ability of the surface to either adhere or repel bacteria based on the pore composition was tested using *S. aureus* as model bacteria. Thus, the surfaces were incubated with fluorescent spherical-shaped *S. aureus* during 1 h. Then, the surfaces were washed and the immobilized bacteria were detected by fluorescence microscopy. The optical images of the porous surfaces and the fluorescence images upon bacterial incubation are depicted in Figure 8. Based on the fluorescence images it is possible to conclude that the presence of PEO inside of the pores clearly influences the adhesion of *S. aureus*. More precisely, blends having 25 wt % of **P2** prevent to a large extent the bacterial immobilization. This preliminary testing demonstrated that these promising functional surfaces may be employed as coatings for membranes that are in contact with water.

CONCLUSIONS

In this Research Article, we demonstrated that polyimide-*g*-PEO copolymers can be readily obtained by polycondensation of dianhydrides and an aromatic diamine containing PEO side groups, applying the classical two-steps method of polyimide synthesis. As a result, combining PEO diamine with other aromatic diamines, copolymers with different content of PEO can be prepared, which show variable hydrophilic content depending on the PEO content. More interestingly, these copolymers were employed in the elaboration of porous structured surfaces by the Breath Figure method. Varying the polymer concentration, the composition of copolymer, and also blending copolymers with variable composition allowed us to prepare well-ordered porous films. In particular, blends of **P1** and **P2**, led to pores with distinct hole and surface composition. Because of the amphiphilic nature of the polyimide-*g*-PEO copolymers employed, they were preferentially located inside of the holes. Moreover, the amount of PEO within the pore could

DOI: 10.1021/acsami.5b01525
ACS Appl. Mater. Interfaces 2015, 7, 9716−9724

be varied depending on the blend composition employed for the preparation of the porous surfaces. Finally, the behavior of these functional porous surfaces against bacterial adhesion was explored. In particular we evidenced that the bacterial immobilization was reduced by using blends having 10% of **P2** and almost completely avoided in the porous films prepared from the blends of 25% of **P2**.

In summary, we evidenced here that bacterial adhesion onto membranes can be prevented using the Breath Figure approach that permits simultaneously the preparation of microstructured porous structures and functional pores containing antifouling PEO segments.

AUTHOR INFORMATION

Corresponding Author

*Email: jrodriguez@ictp.csic.es.

Notes

The authors declare no competing financial interest.

ACKNOWLEDGMENTS

The authors gratefully acknowledge support from the Consejo Superior de Investigaciones Científicas (CSIC). Equally, this work was financially supported by the Ministerio de Economía y Competitividad (MINECO) (Projects MAT2010-17016 and MAT2013-47902-C2-1-R).

REFERENCES

(1) Ostuni, E.; Chen, C. S.; Ingber, D. E.; Whitesides, G. M. Selective Deposition of Proteins and Cells on Arrays of Microwells. *Langmuir* **2001**, *17* (9), 2828−2834.

(2) Joannopoulos, J. D.; Johnson, S. G.; Winn, J. N.; Meade, R. D. *Photonic Crystals: Molding the Flow of Light*, 2nd edition; Princeton University Press: Princeton, NJ, 2008.

(3) You, B.; Shi, L.; Wen, N.; Liu, X.; Wu, L.; Zi, J. A Facile Method for Fabrication of Ordered Porous Polymer Films. *Macromolecules* **2008**, *41* (24), 9952−9952.

(4) Yoshida, M. Novel Thin Film with Cylindrical Nanopores that Open and Close Depending on Temperature: First Successful Synthesis. *Macromolecules* **1996**, *29* (27), 8987−8989.

(5) Bunz, U. H. F. Breath Figures as A Dynamic Templating Method for Polymers and Nanomaterials. *Adv. Mater.* **2006**, *18* (8), 973−989.

(6) Bai, H.; Du, C.; Zhang, A.; Li, L. Breath Figure Arrays: Unconventional Fabrications, Functionalizations, and Applications. *Angew. Chem., Int. Ed.* **2013**, *52* (47), 12240−12255.

(7) Escalé, P.; Rubatat, L.; Billon, L.; Save, M. Recent Advances in Honeycomb-Structured Porous Polymer Films Prepared via Breath Figures. *Eur. Polym. J.* **2012**, *48* (6), 1001−1025.

(8) Hernández-Guerrero, M.; Stenzel, M. H. Honeycomb Structured Polymer Films via Breath Figures. *Polym. Chem.* **2012**, *3* (3), 563−577.

(9) Muñoz-Bonilla, A.; Fernández-García, M.; Rodríguez-Hernández, J. Towards Hierarchically Ordered Functional Porous Polymeric Surfaces Prepared by the Breath Figures Approach. *Prog. Polym. Sci.* **2014**, *39* (3), 510−554.

(10) Hoa, M. L. K.; Lu, M. H.; Zhang, Y. Preparation of Porous Materials With Ordered Hole Structure. *Adv. Coll. Inter. Sci.* **2006**, *121* (1−3), 9−23.

(11) Wu, D.; Xu, F.; Sun, B.; Fu, R.; He, H.; Matyjaszewski, K. Design and Preparation of Porous Polymers. *Chem. Rev.* **2012**, *112* (7), 3959−4015.

(12) Cassagneau, T.; Caruso, F. Conjugated Polymer Inverse Opals for Potentiometric Biosensing. *Adv. Mater.* **2002**, *14* (24), 1837−1841.

(13) Hong, J. C.; Park, J. H.; Chun, C.; Kim, D. Y. Photoinduced Tuning of Optical Stop Bands in Azopolymer Based Inverse Opal Photonic Crystals. *Adv. Funct. Mater.* **2007**, *17* (14), 2462−2469.

(14) You, B.; Shi, L.; Wen, N.; Liu, X.; Wu, L.; Zi, J. A Facile Method for Fabrication of Ordered Porous Polymer Films. *Macromolecules* **2008**, *41* (18), 6624−6626.

(15) Li, C.; Hong, G. S.; Yu, H.; Qi, L. M. Facile Fabrication of Honeycomb-Patterned Thin Films of Amorphous Calcium Carbonate And Mosaic Calcite. *Chem. Mater.* **2010**, *22* (10), 3206−3211.

(16) Zhang, S.; Zhou, S.; You, B.; Wu, L. Fabrication of Ordered Porous Polymer Film via a One-Step Strategy and Its Formation Mechanism. *Macromolecules* **2009**, *42* (10), 3591−3597.

(17) Xue, M. J.; Xiao, W. T.; Zhang, Z. J. Porous Films From Transformation of Polymeric Sphere Arrays. *Adv. Mater.* **2008**, *20* (3), 439−442.

(18) Santos, L.; Martin, P.; Ghilane, J.; Lacaze, P. C.; Randriamahazaka, H.; Abrantes, L. M.; Lacroix, J. C. Electrosynthesis of Well-Organized Nanoporous Poly(3,4-Ethylenedioxythiophene) by Nanosphere Lithography. *Electrochem. Commun.* **2010**, *12* (7), 872−875.

(19) Pietsch, T.; Gindy, N.; Fahmi, A. Nano- and Micro-Sized Honeycomb Patterns Through Hierarchical Self-Assembly of Metal-Loaded Diblock Copolymer Vesicles. *Soft Matter* **2009**, *5* (11), 2188−2197.

(20) Shin, Y.; Li, X. S.; Wang, C.; Coleman, J. R.; Exarhos, G. J. Synthesis of Hierarchical Titanium Carbide from Titania-Coated Cellulose Paper. *Adv. Mater.* **2004**, *16* (14), 1212−1215.

(21) Shin, Y.; Wang, C.; Exarhos, G. J. Synthesis of SiC Ceramics by the Carbothermal Reduction of Mineralized Wood With Silica. *Adv. Mater.* **2005**, *17* (1), 73−77.

(22) Huang, J.; Kunitake, T. Nano-Precision Replication of Natural Cellulosic Substances by Metal Oxides. *J. Am. Chem. Soc.* **2003**, *125* (39), 11834−11835.

(23) Meldrum, F.; Seshadri, R. Porous Gold Structures Through Templating by Echinoid Skeletal Plates. *Chem. Commun.* **2000**, *1*, 29−30.

(24) Luo, R. L.; Young, T. H.; Sun, Y. M. Structure Formation and Characterization of EVAL Membranes With Cosolvent of Isopropanol and Water. *Polymer* **2003**, *44* (1), 157−166.

(25) Zhang, Y. L.; Ding, H.; Wei, S.; Liu, S.; Wang, Y. P.; Xiao, F. S. Hierarchical Macroporous Epoxy Resin Templated from Single Semi-Fluorinated Surfactant. *J. Porous Mater.* **2010**, *17* (6), 693−698.

(26) Tang, C. B.; Bang, J.; Stein, G. E.; Fredrickson, G. H.; Hawker, C. J.; Kramer, E. J.; Sprung, M.; Wang, J. Square Packing and Structural Arrangement of ABC Triblock Copolymer Spheres in Thin Films. *Macromolecules* **2008**, *41* (12), 4328−4339.

(27) Xiang, H.; Lin, Y.; Russell, T. P. Electrically Induced Patterning in Block Copolymer Films. *Macromolecules* **2004**, *37* (14), 5358−5363.

(28) Morikawa, Y.; Nagano, S.; Watanabe, K.; Kamata, K.; Iyoda, T.; Seki, T. Optical Alignment and Patterning of Nanoscale Microdomains in A Block Copolymer Thin Film. *Adv. Mater.* **2006**, *18* (7), 883−886.

(29) Li, G.; Burggraf, L. W. Controlled Patterning of Polymer Films Using an AFM Tip as a Nano-Hammer. *Nanotechnology* **2007**, *18* (24), No. 245302.

(30) Behl, M.; Seekamp, J.; Zankovych, S.; Sotomayor Torres, C. M.; Zentel, R.; Ahopelto, J. Towards Plastic Electronics: Patterning Semiconducting Polymers by Nanoimprint Lithography. *Adv. Mater.* **2002**, *14* (8), 588−591.

(31) Campbell, M.; Sharp, D. N.; Harrison, M. T.; Denning, R. G.; Turberfield, A. J. Fabrication of Photonic Crystals for the Visible Spectrum by Holographic Lithography. *Nature* **2000**, *404* (6773), 53−56.

(32) Nishikawa, T.; Ookura, R.; Nishida, J.; Arai, K.; Hayashi, J.; Kurono, N.; Sawadaishi, T.; Hara, M.; Shimomura, M. Fabrication of Honeycomb Film of an Amphiphilic Copolymer at the Air−Water Interface. *Langmuir* **2002**, *18* (15), 5734−5740.

(33) Stenzel, M. H. Formation of Regular Honeycomb-Patterned Porous Film by Self-Organization. *Aust. J. Chem.* **2002**, *55* (4), 239−243.

(34) Connal, L. A.; Gurr, P. A.; Qiao, G. G.; Solomon, D. H. From Well Defined Star-Microgels to Highly Ordered Honeycomb Films. *J. Mater. Chem.* **2005**, *15* (12), 1286−1292.

DOI: 10.1021/acsami.5b01525
ACS Appl. Mater. Interfaces 2015, 7, 9716−9724

(35) Srinivasarao, M.; Collings, D.; Philips, A.; Patel, S. Three-Dimensionally Ordered Array of Air Bubbles in a Polymer Film. *Science* **2001**, *292* (5514), 79−83.
(36) Widawski, G.; Rawiso, M.; François, B. Self-Organized Honeycomb Morphology of Star-Polymer Polystyrene Films. *Nature* **1994**, *369* (6479), 387−389.
(37) Vakuliuk, P.; Burban, A.; Konovalova, V.; Bryk, M.; Vortman, M.; Klymenko, N.; Shevchenko, V. Modified Track Membranes with Antibacterial Properties. *Desalination* **2009**, *235* (1−3), 160−169.
(38) Lindau, J.; Jönsson, A. S. Adsorptive Fouling of Modified and Unmodified Commercial Polymeric Ultrafiltration Membranes. *J. Membr. Sci.* **1999**, *160* (1), 65−76.
(39) Tashiro, T. Antibacterial and Bacterium Adsorbing Macromolecules. *Macromol. Mater. Eng.* **2001**, *286* (2), 63−87.
(40) Appendini, P.; Hotchkiss, J. H. Surface Modification of Poly(Styrene) by The Attachment of An Antimicrobial Peptide. *J. Appl. Polym. Sci.* **2001**, *81* (3), 609−616.
(41) Tiller, J. C.; Lee, S. B.; Lewis, K.; Klibanov, A. M. Polymer Surfaces Derivatized with Poly(Vinyl-N-Hexylpyridinium) Kill Airborne and Waterborne Bacteria. *Biotechnol. Bioeng.* **2002**, *79* (4), 465−471.
(42) Tiller, J. C.; Liao, C.-J.; Lewis, K.; Klibanov, A. M. Designing Surfaces that Kill Bacteria on Contact. *Proc. Natl. Acad. Sci. U. S. A.* **2001**, *98* (11), 5981−5985.
(43) Yu, H.; Cao, Y.; Kang, G.; Liu, J.; Li, M.; Yuan, Q. Enhancing Antifouling Property of Polysulfone Ultrafiltration Membrane by Grafting Zwitterionic Copolymer via UV-Initiated Polymerization. *J. Membr. Sci.* **2009**, *342* (1−2), 6−13.
(44) Yue, W.-W.; Li, H.-J.; Xiang, T.; Qin, H.; Sun, S.-D.; Zhao, C.-S. Grafting of Zwitterion from Polysulfone Membrane via Surface-Initiated ATRP with Enhanced Antifouling Property and Biocompatibility. *J. Membr. Sci.* **2013**, *446*, 79−91.
(45) Xie, Y.-j.; Yu, H.-y.; Wang, S.-y.; Xu, Z.-k. Improvement of Antifouling Characteristics in a Bioreactor of Polypropylene Microporous Membrane by the Adsorption of Tween 20. *J. Environ. Sci.-China* **2007**, *19* (12), 1461−1465.
(46) Manniso, J. L. Microporous Anti-Fouling Marine Coating. U.S. PatentUS 4865909 A, 1989.
(47) Lowe, S.; O'Brien-Simpson, N. M.; Connal, L. A. Antibiofouling Polymer Interfaces: Poly(Ethylene Glycol) and Other Promising Candidates. *Polym. Chem.* **2015**, *6*, 198−212.
(48) Konradi, R.; Acikgoz, C.; Textor, M. Polyoxazolines for Nonfouling Surface Coatings—A Direct Comparison to the Gold Standard PEG. *Macromol. Rapid Commun.* **2012**, *33* (19), 1663−1676.
(49) Knop, K.; Hoogenboom, R.; Fischer, D.; Schubert, U. S. Poly(Ethylene Glycol) in Drug Delivery: Pros and Cons as Well as Potential Alternatives. *Angew. Chem., Int. Ed.* **2010**, *49* (36), 6288−6308.
(50) Park, J. Y.; Acar, M. H.; Akthakul, A.; Kuhlman, W.; Mayes, A. M. Polysulfone-Graft-Poly(Ethylene Glycol) Graft Copolymers for Surface Modification of Polysulfone Membranes. *Biomaterials* **2006**, *27* (6), 856−865.
(51) Xu, Z.-K.; Nie, F.-Q.; Qu, C.; Wan, L.-S.; Wu, J.; Yao, K. Tethering Poly(Ethylene Glycol)s to Improve the Surface Biocompatibility of Poly(Acrylonitrile-Co-Maleic Acid) Asymmetric Membranes. *Biomaterials* **2005**, *26* (6), 589−598.
(52) Prince, J. A.; Bhuvana, S.; Boodhoo, K. V. K.; Anbharasi, V.; Singh, G. Synthesis And Characterization of PEG-Ag Immobilized PES Hollow Fiber Ultrafiltration Membranes with Long Lasting Antifouling Properties. *J. Membr. Sci.* **2014**, *454* (0), 538−548.
(53) Yu, H.-J.; Cao, Y.-M.; Kang, G.-D.; Zhou, M.-Q.; Liu, J.-H.; Yuan, Q. Enhancing Antifouling Property of Polysulfone Ultrafiltration Membrane by Grafting Poly(Ethylene Glycol) Methyl Ether Methacrylate(PEGMA) via UV-Initiated Polymerization. *Chem. Res. Chin. Univ.* **2010**, *31* (12), 2506−2510.
(54) Yu, H. Y.; Hu, M. X.; Xu, Z. K.; Wang, J. L.; Wang, S. Y. Surface Modification of Polypropylene Microporous Membranes to Improve their Antifouling Property in MBR: NH_3 Plasma Treatment. *Sep. Purif. Technol.* **2005**, *45* (1), 8−15.
(55) Yu, H. Y.; Xie, Y.; Hu, M. X.; Wang, J. L.; Wang, S. Y.; Xu, Z. K. Surface Modification of Polypropylene Microporous Membrane to Improve its Antifouling Property in MBR: CO_2 Plasma Treatment. *J. Membr. Sci.* **2005**, *254* (1−2), 219−227.
(56) Yu, H.-Y.; He, X.-C.; Liu, L.-Q.; Gu, J.-S.; Wei, X.-W. Surface Modification of Polypropylene Microporous Membrane to Improve its Antifouling Characteristics in an SMBR: N-2 Plasma Treatment. *Water Res.* **2007**, *41* (20), 4703−4709.
(57) Yu, H.-Y.; Liu, L.-Q.; Tang, Z.-Q.; Yan, M.-G.; Gu, J.-S.; Wei, X.-W. Mitigated Membrane Fouling in an SMBR by Surface Modification. *J. Membr. Sci.* **2008**, *310* (1−2), 409−417.
(58) Zhan, J.; Liu, Z.; Wang, B. G.; Ding, F. X. Modification of A Membrane Surface Charge by a Low Temperature Plasma Induced Grafting Reaction and its Application to Reduce Membrane Fouling. *Sep. Sci. Technol.* **2004**, *39* (13), 2977−2995.
(59) Yu, H.-Y.; Liu, L.-Q.; Tang, Z.-Q.; Yan, M.-G.; Gu, J.-S.; Wei, X.-W. Surface Modification of Polypropylene Microporous Membrane to Improve its Antifouling Characteristics in an SMBR: Air Plasma Treatment. *J. Membr. Sci.* **2008**, *311* (1−2), 216−224.
(60) Abajo González, J. d.; Campa, J. G. d. l.; Carretero, P.; Lozano, Á. E.; Molina, S.; Teli, S. B. Hydrophilic Porous Asymmetric Ultrafiltration Membranes of Aramid-G-PEO Copolymers. *J. Membr. Sci.* **2014**, *454* (1), 233−242.
(61) Liu, Y.; Wang, L.; Han, X. Self-Assembly Fabrication of Ordered Microporous Films from a Soluble Polyimide Modified by Methyl Groups Based on Breath Figures. *Desalin. Water Treat.* **2013**, *51* (25−27), 5107−5112.
(62) Han, X. T.; Tian, Y.; Wang, L. H.; Xiao, C. F. Formation of Honeycomb Films Based on a Soluble Polyimide Synthesized From 2,2′-Bis 4-(3,4-Dicarboxyphenoxy)Phenyllhexafluoropropane Dianhydride and 3,3′-Dimethyl-4,4′-Diaminodiphenylmethane. *J. Appl. Polym. Sci.* **2008**, *107* (1), 618−623.
(63) Wang, L. H.; Tian, Y.; Ding, H. Y.; Liu, B. Q. Formation of Ordered Macroporous Films from Fluorinated Polyimide by Water Droplets Templating. *Eur. Polym. J.* **2007**, *43* (3), 862−869.
(64) Tian, Y.; Liu, S.; Ding, H.; Wang, L.; Liu, B.; Shi, Y. Formation of Deformed Honeycomb-Patterned Films from Fluorinated Polyimide. *Polymer* **2007**, *48* (8), 2338−2344.
(65) Yabu, H.; Tanaka, M.; Ijiro, K.; Shimomura, M. Preparation of Honeycomb-Patterned Polyimide Films by Self-Organization. *Langmuir* **2003**, *19* (15), 6297−6300.
(66) Carretero, P.; Molina, S.; Sandín, R.; Rodríguez-Hernández, J.; Lozano, A. E.; Abajo, J. d. Hydrophilic Polyisophthalamides Containing Poly(Ethylene Oxide) Side Chains: Synthesis, Characterization and Physical Properties. *J. Polym. Sci., Part A: Polym. Chem.* **2013**, *51* (4), 963−976.

DOI: 10.1021/acsami.5b01525
ACS Appl. Mater. Interfaces 2015, 7, 9716−9724